
Designing a Conditional Prior Distribution for Flow-Based Generative Models

Noam Issachar^{*1} Mohammad Salama^{*1} Raanan Fattal¹ Sagie Benaim¹

Abstract

Flow-based generative models have recently shown impressive performance for conditional generation tasks, such as text-to-image generation. However, current methods transform a general unimodal noise distribution to a specific mode of the target data distribution. As such, every point in the initial source distribution can be mapped to every point in the target distribution, resulting in long average paths. To this end, in this work, we tap into a non-utilized property of conditional flow-based models: the ability to design a non-trivial prior distribution. Given an input condition, such as a text prompt, we first map it to a point lying in data space, representing an “average” data point with the minimal average distance to all data points of the same conditional mode (e.g., class). We then utilize the flow matching formulation to map samples from a parametric distribution centered around this point to the conditional target distribution. Experimentally, our method significantly improves training times and generation efficiency (FID, KID and CLIP alignment scores) compared to baselines, producing high quality samples using fewer sampling steps.

1. Introduction

Conditional generative models are of significant importance for many scientific and industrial applications. Of these, the class of flow-based models and score-based diffusion models has recently shown a particularly impressive performance (Lipman et al., 2022; Esser et al., 2024; Dhariwal & Nichol, 2021; Ho & Salimans, 2022). Although impressive, current methods suffer from long training and sampling times. To this end, in this work, we tap into a non-utilized property of conditional flow-based models: the ability to design a non-trivial prior distribution for conditional flow-based models based on the input condition. In particular, for

class-conditional generation and text-to-image generation, we propose a *robust* method for constructing a conditional flow-based generative model using an informative condition-specific prior distribution fitted to the conditional modes (e.g., classes) of the target distribution. By better modeling the prior distribution, we aim to improve the efficiency, both at training and at inference, of conditional generation via flow matching, thus achieving high quality results with fewer sampling steps.

Given an input variable (e.g., a class or text prompt), current flow-based and score-based diffusion models combine the input condition with intermediate representations in a learnable manner. However, crucially, these models are still trained to transform a generic unimodal noise distribution to the different modes of the target data distribution. In some formulations, such as score-based diffusion (Ho et al., 2020b; Song et al., 2020; Sohl-Dickstein et al., 2015), the use of a Gaussian source density is intrinsically connected to the process constructing the transformation. In others, such as flow matching (Lipman et al., 2022; Liu et al., 2022; Albergo & Vanden-Eijnden, 2022), a Gaussian source is not required, but is often chosen as a default for convenience. Consequently, in these settings, the prior distribution bears little or no resemblance to the target, and hence every point in the initial source distribution can be mapped to every point in every mode in the target distribution, corresponding to a given condition. This means that the average distance between pairs of source-target points is fairly large.

In the unconditional setting, recent works (Pooladian et al., 2023; Tong et al., 2023), show that starting from a source (noise) data point that is close to the target data sample, during training, results in straighter probability flow lines, fewer sampling steps at test time, and faster training time. This is in comparison to the non-specific random pairing between the distributions typically used for training flow-based and score-based models. This suggests that finding a strategy to minimize the average distance between source and target points could result in a similar benefit. Our work aims to construct this by constructing a *condition-specific* source distribution by leveraging the input condition.

We, therefore, propose a novel paradigm for designing an informative condition-specific prior distribution for a flow-based conditional generative model. While in this work, we

^{*}Equal contribution ¹School of Computer Science and Engineering, The Hebrew University of Jerusalem, Israel. Correspondence to: Noam Issachar <noam.issachar@mail.huji.ac.il>.

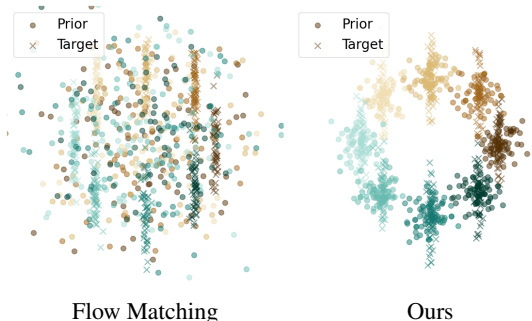


Figure 1. An illustration of our approach. The LHS illustrates the standard flow matching paradigm, where every sample in the source Gaussian distribution (shown as a circular point) can be mapped to every sample in the conditional target mode (shown as a cross point), where each class samples are shown in a different color. In contrast, our method, shown on the RHS, constructs a class-specific conditional distribution as a source prior distribution. Each sample in the source distribution is, on average, closer to its corresponding sample in the target mode.

choose to work on *flow matching*, our approach can also be incorporated in other generative models, supporting arbitrary prior distributions. In the first step, we embed the input condition c to a point x_c lying in data space (which can be a latent one). For a discrete set of classes, this is done by averaging training samples corresponding to a given class c in the data space. In the continuous case, such as text-to-image, we first choose a meaningful embedding for the input condition c (e.g. CLIP (Radford et al., 2021)). Given a training sample x_c and the corresponding conditional embedding e_c , we train a deterministic mapper function that projects e_c to x_c lying in data space. This results in an “average” data point of all samples x corresponding to the condition c . To enable stochastic mapping, we then map samples from a parametric conditional distribution centered on x_c to the conditional target distribution $\rho_1(x|c)$.

While our approach can be implemented with any parametric conditional distribution, in our experiments, we chose to utilize a Gaussian Mixture Model (GMM). Specifically, the mean of each Gaussian is the “average” conditional data point. In the discrete condition case, each prior-Gaussian’s covariance is estimated directly from the class-dependent training data, while for the continuous setting, it is fixed as a hyperparameter. Further, while the data space can be arbitrary, we choose it as the latent space of a pre-trained variational autoencoder (VAE). These choices are derived from the following desirable properties: (i). One can easily sample from a GMM, (ii). Class conditional information can be directly represented by a GMM, with each Gaussian corresponding to a conditional mode. (iii). We find empirically (see Sec. 4.2), for real-world distributions (ImageNet (Deng et al., 2009) and MS-COCO (Lin et al., 2014)), that the average distance between pairs of samples from the prior and data distributions (*i.e.* the *transport cost*) is

much smaller than the unimodal Gaussian alternative (as in (Lipman et al., 2022; Pooladian et al., 2023)). Moreover, previous works (Jiang et al., 2017; Bull et al., 2021; Hinton & Salakhutdinov, 2006) has shown that applying a GMM in a VAE space can be highly effective for clustering, suggesting that it can act as a suitable prior distribution. An illustration of our approach, for a simple setting consisting of eight Gaussians, each representing a different class, is shown in Fig. 1.

To validate our approach, we first formulate flow matching from our conditional prior distribution (CPD) and show that our formulation results in low global truncation errors. Next, we consider a toy setting with a known analytical target distribution and illustrate our method’s advantage in efficiency and quality. For real-world datasets, we consider both the MS-COCO (text-to-image generation) and ImageNet-64 datasets (class conditioned generation). Compared to other flow-based (CondOT (Lipman et al., 2022), BatchOT (Pooladian et al., 2023)) and diffusion (DDPM (Ho et al., 2020a)) based models, our approach allows for faster training and sampling, as well as for a significantly improved generated image quality and diversity, evaluated using FID and KID, and alignment to the input text, evaluated using CLIP score.

2. Related Work

Flow-based Models. Continuous Normalizing Flows (CNFs) (Chen et al., 2019) emerged as a novel paradigm in generative modeling, offering a continuous-time extension to the discrete Normalizing Flows (NF) framework (Kobyzev et al., 2020; Papamakarios et al., 2021). Recently, Flow Matching (Lipman et al., 2022; Liu et al., 2022; Albergo & Vanden-Eijnden, 2022) has been introduced as a simulation-free alternative for training CNFs. In scenarios involving conditional data (e.g., in text-to-image generation), conditioning is applied similarly to diffusion models, often through cross attention between the input condition and latent features. Typically, the source distribution remains unimodal, like a standard Gaussian (Liu et al., 2024). In contrast, our approach derives a prior distribution that is dependent on the input condition.

Informative Prior Design. Designing useful prior distribution has been well studied in generative models such as VAEs (e.g., (Dilokthanakul et al., 2016)) and Normalizing Flows (e.g., (Izmailov et al., 2020)) In the context of score-based models and flow matching, several works designed informative priors. For score-based diffusion, (Lee et al., 2021) has introduced an approach of formulating the diffusion process using a non-standard Gaussian, where the Gaussian’s statistics are determined by the conditional distribution statistics. However, this approach is constrained by the use of a Gaussian prior, which limits its flexibility. Recently, (Pooladian et al., 2023; Tong et al., 2023)

constructed a prior distribution by utilizing the dynamic optimal transport (OT) formulation across mini-batches during training. Despite impressive capabilities such as efficient sampling (minimizing trajectory intersections), they suffer from several drawbacks: (i). Highly expensive training: Computing the optimal transport solution requires quadratic time and memory, which is not applicable to large mini-batches and high dimensional data. (ii). When dealing with high dimensional data, the effectiveness of this formulation decreases dramatically. An increase in performance requires an exponential increase in batch-size in relation to data dimension. Our approach avoids these limitations by leveraging the conditioning variable of the data distribution.

3. Preliminaries

We begin by introducing Continuous Normalizing Flow (Chen et al., 2019) in Sec. 3.1 and Flow Matching (Lipman et al., 2022) in Sec. 3.2. This will motivate our approach, detailed in Sec. 4, which defines an informative conditional prior distribution on a conditional flow model.

3.1. Continuous Normalizing Flows

A probability density function over a manifold \mathcal{M} is a continuous non-negative function $\rho : \mathcal{M} \rightarrow \mathbb{R}_+$ such that $\int \rho(x)dx = 1$. We set \mathcal{P} to be the space of such probability densities on \mathcal{M} . A *probability path* $\rho_t : [0, 1] \rightarrow \mathcal{P}$ is a curve in probability space connecting two densities $\rho_0, \rho_1 \in \mathcal{P}$ at endpoints $t = 0, t = 1$. A *flow* $\psi_t : [0, 1] \times \mathcal{M} \rightarrow \mathcal{M}$ is a time-dependent diffeomorphism defined to be the solution to the Ordinary Differential Equation (ODE):

$$\frac{d}{dt}\psi_t(x) = u_t(\psi_t(x)), \quad \psi_0(x) = x \quad (1)$$

subject to initial conditions where $u_t : [0, 1] \times \mathcal{M} \rightarrow \mathcal{TM}$ is a time-dependent smooth vector field on the collection of all tangent planes on the manifold \mathcal{TM} (*tangent bundle*). A flow ψ_t is said to generate a probability path ρ_t if it ‘pushes’ ρ_0 forward to ρ_1 following the time-dependent vector field u_t . The path is denoted by:

$$\rho_t = [\psi_t]_{\#}\rho_0 := \rho_0(\psi_t^{-1}(x)) \det \left| \frac{d\psi_t^{-1}}{dx}(x) \right| \quad (2)$$

where $\#$ is the standard push-forward operation. Previously, (Chen et al., 2019) proposed to model the flow ψ_t implicitly by parameterizing the vector field u_t , to produce ρ_t , in a method called *Continuous Normalizing Flows* (CNF).

3.2. Flow Matching

Flow Matching (FM) (Lipman et al., 2022) is a simulation-free method for training CNFs that avoids likelihood computation during training, which can be expensive. It does

so by fitting a vector field v_t^θ with parameters θ and regressing vector fields u_t that are known *a priori* to generate a probability path $\rho_t \in \mathcal{P}$ satisfying the boundary conditions:

$$\rho_0 = p, \quad \rho_1 = q \quad (3)$$

Note that u_t is generally intractable. However, a key insight of (Lipman et al., 2022), is that this vector field can be constructed based on conditional vector fields $u_t(x|x_1)$ that generate conditional probability paths $\rho_t(x|x_1)$. The push-forward of the conditional flow $\psi_t(x|x_1)$, start at ρ_t and concentrate the density around $x = x_1 \in \mathcal{M}$ at $t = 1$. Marginalizing over the target distribution q recovers the unconditional probability path and unconditional vector field:

$$\rho_t(x) = \int_{\mathcal{M}} \rho_t(x|x_1)q(x_1)dx_1 \quad (4)$$

$$u_t(x) = \int_{\mathcal{M}} u_t(x|x_1) \frac{\rho_t(x|x_1)q(x_1)}{\rho_t(x)} dx_1 \quad (5)$$

This vector field can be matched by a parameterized vector field v_θ using the $\mathcal{L}_{\text{cfm}}(\theta)$ objective:

$$\mathbb{E}_{t \sim \mathcal{U}(0,1), q(x_1), \rho_t(x|x_1)} \|v_\theta(t, x) - u_t(x|x_1)\|^2 \quad (6)$$

where $\|\cdot\|$ is a norm on \mathcal{TM} . One particular choice of a conditional probability path $\rho_t(x|x_1)$ is to use the flow corresponding the optimal transport displacement interpolant (McCann, 1997) between Gaussian distributions. Specifically, in the context of the conditional probability path, $\rho_0(x|x_1)$ is the standard Gaussian, a common convention in generative modeling, and $\rho_1(x|x_1)$ is a small Gaussian centered around x_1 . The conditional flow interpolating these distributions is given by:

$$x_t = \psi_t(x|x_1) = (1-t)x_0 + tx_1 \quad (7)$$

which results in the following conditional vector field:

$$u_t(x|x_1) = \frac{x_1 - x}{1-t} \quad (8)$$

which is marginalized in Eq. 6. Substituting Eq. 7 to Eq. 8, one can also express the value of this vector field using a simpler expression:

$$u_t(x_t|x_1) = x_1 - x_0 \quad (9)$$

Conditional Generation via Flow Matching. Flow matching (FM) has been extended to conditional generative modeling in several works (Zheng et al., 2023; Dao et al., 2023; Atanackovic et al., 2024; Isobe et al., 2024). In contrast to the original FM formulation of Eq. 8, one first samples a condition c . One then produces samples from $\rho_t(x|c)$ by passing c as input to the parametric vector field

v_θ . The *Conditional Generative Flow Matching* (CGFM) objective $\mathcal{L}_{\text{cgfm}}(\theta)$ is:

$$\mathbb{E}_{t \sim \mathcal{U}(0,1), q(x_1, c), \rho_t(x|x_1)} \|v_\theta(t, c, x) - u_t(x|x_1)\|^2 \quad (10)$$

In practice, c is incorporated by embedding it into some representation space and then using cross-attention between it and the features of v_θ as in (Rombach et al., 2022).

Flow Matching with Joint Distributions. While (Lipman et al., 2022) considered the setting of independently sampled x_0 and x_1 , recently, (Pooladian et al., 2023; Tong et al., 2023) generalized the FM framework to an arbitrary joint distribution of $\rho(x_0, x_1)$ in the unconditional generation setting. This construction satisfies the following marginal constraints, i.e.

$$\int \rho(x_0, x_1) dx_1 = q(x_0), \int \rho(x_0, x_1) dx_0 = q(x_1) \quad (11)$$

Pooladian et al. (2023) modified the conditional probability path construction so at $t = 0$, $\rho_0(x_0|x_1) = p(x_0|x_1)$, where $p(x_0|x_1)$ is the conditional distribution $\frac{\rho(x_0, x_1)}{q(x_1)}$. The *Joint Conditional Flow Matching* (JCFM) objective is:

$$\mathcal{L}_{\text{jcfm}}(\theta) = \mathbb{E}_{t \sim \mathcal{U}(0,1), \rho(x_0, x_1)} \|v_\theta(t, x) - u_t(x|x_1)\|^2 \quad (12)$$

4. Method

Given a set $\{x_{1_i}, c_i\}_{i=1}^m$ of input samples and their corresponding conditioning states, our goal is to construct a flow-matching model that samples from $q(x_1|c)$ that start from our conditional prior distribution (CPD).

4.1. Flow Matching from Conditional Prior Distribution

We generalize the framework of Sec. 3.2 to a construction that uses an arbitrary conditional joint distribution of $\rho(x_0, x_1, c)$ which satisfy the marginal constraints:

$$\int \rho(x_0, x_1, c) dx_0 = q(x_1, c), \int \rho(x_0, x_1, c) dx_1 dc = p(x_0)$$

Then, building on flow matching, we propose to modify the conditional probability path so that at $t = 0$, we define:

$$\rho_0(x_0|x_1, c) = p(x_0|x_1, c) \quad (13)$$

where $p(x_0|x_1, c)$ is the conditional distribution $\frac{\rho(x_0, x_1, c)}{q(x_1, c)}$. Using this construction, we satisfy the boundary condition of Eq. 3:

$$\rho_0(x_0) = \int \rho_0(x_0|x_1, c) q(x_1, c) dx_1 dc \quad (14)$$

$$= \int p(x_0|x_1, c) dx_1 dc = p(x_0) \quad (15)$$

The conditional probability path $\rho_t(x|x_1, c)$ does not need to be explicitly formulated. Instead, only its corresponding conditional vector field $u_t(x|x_1, c)$ needs to be defined such that points x_0 drawn from the conditional prior distribution $\rho_0(x_0|x_1, c)$, reach x_1 at $t = 1$, i.e., reach distribution $\rho_1(x|x_1, c) = \delta(x - x_1)$. We thus purpose the *Conditional Generation Joint FM* $\mathcal{L}_{\text{cgjfm}}(\theta)$ objective:

$$\mathbb{E}_{t \sim \mathcal{U}(0,1), q(x_0, x_1, c)} \|v_\theta(t, x, c) - u_t(x|x_1, c)\|^2 \quad (16)$$

where $x = \psi_t(x_0|x_1, c)$. Training only involves sampling from $q(x_0, x_1, c)$ and does not require explicitly defining the densities $q(x_0, x_1, c)$ and $\rho_t(x|x_1, c)$. We note that this objective is reduced to the CGFM objective Eq. 10 when $q(x_0, x_1, c) = q(x_1, c)p(x_0)$.

4.2. Conditional Prior Distribution

We now describe our choice of a condition-specific prior distribution. When choosing a conditional prior distribution we want to adhere to the following design principles: (i) *Easy to sample*: can be efficiently sampled from. (ii) *Well represents the target conditional modes*. We design a condition-specific prior distribution based on a parametric *Mixture Model* where each mode of the mixture is correlated to a specific conditional distribution $p(x_1|c)$. Specifically, we choose the prior distribution to be the following, *easy to sample*, *Gaussian Mixture Model* (GMM):

$$p_0 = \text{GMM}(\mathcal{N}(\mu_i, \Sigma_i)_{i=1}^n, \pi) \quad (17)$$

where $\pi \in \mathbb{R}^n$ is a probability vector associated with the number of conditions n (could be ∞) and μ_i, Σ_i are parameters determined by the conditional distribution $q(x_1|c_i)$ statistics, i.e.

$$\mu_i = \mathbb{E}[x_1|c_i], \quad \Sigma_i = \text{cov}[x_1|c_i] \quad (18)$$

To sample from the marginal distribution $p(x_0|x_1, c_i)$, we sample from the cluster $\mathcal{N}(\mu_i, \Sigma_i)$ associated with the condition c_i .

Obtaining a Lower Global Truncation Error. Our CPD fits a GMM to the data distribution in a favorable setting, where the association between samples and clusters is given.

In this process, we fit a dedicated Gaussian distribution to data points with the same condition. If the latter are close to being unimodal, this approximation is expected to be tight, in terms of the average distances between samples from the condition data mode and the fitted Gaussian. Tab. 1 provides the average distances between pairs of samples from the prior and data distributions (i.e. the *transport cost*) of CondOT (Lipman et al., 2022), BatchOT (Pooladian et al., 2023) and our CPD over the ImageNet-64 (Deng et al., 2009) and MS-COCO (Lin et al., 2014) datasets. As expected, BatchOT which minimizes this exact measure within mini-batches, obtains better scores than the naïve pairing used

Table 1. Average distances between pairs of samples from the prior and data distributions (i.e. transport cost) on the ImageNet-64 and MS-COCO datasets across baselines.

	ImageNet-64	MS-COCO
CondOT	640	630
BatchOT	632	604
Ours	570	510

in CondOT, while our CPD, which approximates the data using a GMM exploits the conditioning available in these datasets, and obtains considerably lower average distances.

As noted in (Pooladian et al., 2023), lower transport cost is generally associated with straighter flow trajectories, more efficient sampling and lower training time. We want to substantiate this claim from the viewpoint of cumulative errors in numerical integration. Sampling from flow-based models consists of solving a time-dependent ODE of the form $\dot{x}_t = u_t(x_t)$, where u_t is the velocity field. This equation is solved by the following integral $x_t = \int_0^t u_s(x_s) ds$, where the initial condition x_0 is sampled from the prior distribution. Numerical integration over discrete time steps accumulate an error at each step n which is known as the *local truncation error* τ_n , which accumulates into what is known as the *global truncation error* e_n . This error is bounded by (Süli & Mayers, 2003)

$$|e_n| \leq \frac{\max_j \tau_j}{hL} (e^{L(t_n - t_0)} - 1) \quad (19)$$

where h is the step size and L is the Lipschitz constant of the velocity u_t . Accordingly, the distance between the endpoints of a path $\Delta = |x_1 - x_0|$ is given by $|\int_0^1 u_s(x_s) ds|$ which can be interpreted as the magnitude of the average velocity along the path x_t . Hence, the longer the path Δ is, the larger the integrated flow vector field u_t is. For example, if we scale a path uniformly by a factor $C > 1$, i.e., $x_t \rightarrow C(x_t)$, we get, $\frac{d}{dt} C(x_t) = C(u_t)$ in which case the Lipschitz constant L is also multiplied by C .

By shortening the distance between the prior and data distribution, as our CPD does, we lower the integration errors which permits the use of coarser integration steps, which in turn yield smaller global errors. Thus, our construction allows for fewer integration steps during sampling.

4.2.1. CONSTRUCTION

Next, we explain how we construct p_0 (Eq. 17) for both the discrete case (e.g., class conditional generation) and continuous case (e.g., text conditional generation).

Discrete Condition. In the setup of discrete conditional generation, we are given data $\{x_{1_i}, c_i\}_{i=1}^m$ where there are a finite set of conditions c_i . We approximate the statistics of Eq. 18 using the training data statistics. That is, we compute

the mean and covariance matrix of each class (potentially in some latent representation of a pretrained auto-encoder). Since the classes at inference time are the same as in training, we use the same statistics at inference.

Continuous Condition. While in the discrete case we can directly approximate the statistics in Eq. 18 from the training data, in the continuous case (e.g. text-conditional) we need to find those statistics also for conditions that were not seen during training. To this end, we first consider a joint representation space for training samples $\{x_{1_i}, c_i\}_{i=1}^m$, which represents the semantic distances between the conditions c_i and the samples x_{1_i} . In the setting where c_i is text, we choose a pretrained CLIP embedding. c_i is then mapped to this representation space, and then mapped to the data space (which could be a latent representation of an auto-encoder), using a learned mapper \mathcal{P}_θ . Specifically, \mathcal{P}_θ is trained to minimize the objective:

$$\mathcal{L}_{\text{prior}}(\theta) = \mathbb{E}_{q(x_1, c)} \|\mathcal{P}_\theta(E(c)) - x_1\|_2^2, \quad (20)$$

where E is the pre-trained mapping to the joint condition-sample space (e.g. CLIP). \mathcal{P}_θ can be seen as approximating $\mathbb{E}[x_1|c]$, which is used as the mean for the condition specific Gaussian. At inference, where new conditions (e.g., texts) may appear, we first encode the condition c_i to the joint representation space (e.g., CLIP) followed by \mathcal{P}_θ . This mapping provides us with the center μ_i of each Gaussian. We also define $\Sigma_i = \sigma_i^2 \mathbf{I}$ where σ_i is a hyper-parameter, ablated in Sec. 5.2.1

4.3. Training and Inference

Given the prior p_0 (either using the data statistics or by training \mathcal{P}_θ), for each condition c , we have its associated Gaussian parameters μ_c and Σ_c . The map $\psi_t(x|x_1, c)$ must be defined in order to minimize Eq. 16 above. This corresponds to the interpolating maps between this Gaussian at $t = 0$ and a small Gaussian around x_1 at $t = 1$, defined by:

$$\psi_t(x|x_1, c) = \sigma_t(x_1, c)x + \mu_t(x_1, c), \quad (21)$$

$$\sigma_t(x_1, c) = t(\sigma_{\min} \mathbf{I}) + (1-t)\Sigma_c^{1/2}, \quad \text{and} \quad (22)$$

$$\mu_t(x_1, c) = tx_1 + (1-t)\mu_c. \quad (23)$$

This results in the following target flow vector field

$$u_t(\psi_t(x|x_1, c)) = \frac{d}{dt} \psi_t(x|x_1, c) = (\sigma_{\min} \mathbf{I} - \Sigma_c^{1/2})x + x_1 - \mu_c.$$

During inference we are given a condition c and want to sample from $q(x_1|c)$. Similarly to the training, we sample $x_0 \sim p(x_0|c)$ and solve the ODE

$$\frac{d}{dt} \psi_t(x) = v_\theta(t, \psi_t(x), c), \quad \psi_0(x) = x_0 \quad (24)$$

Training and implementation details are in the appendix.

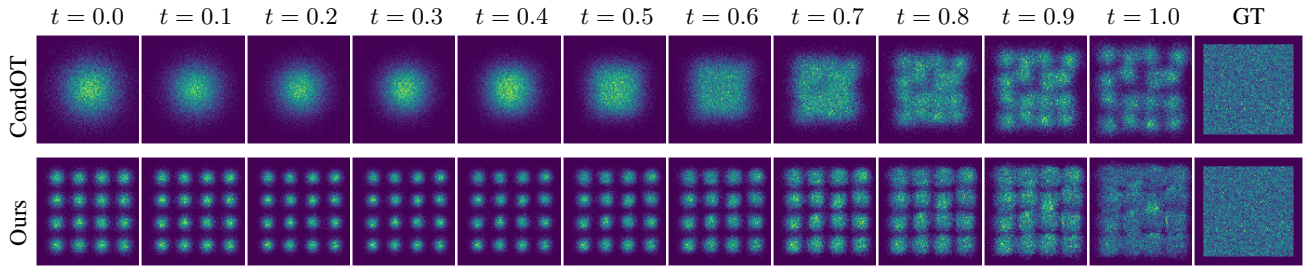


Figure 2. **Trajectory illustration.** A toy example illustrating the trajectory from the source to the target distribution for our method and conditional flow matching using optimal transport (CondOT).

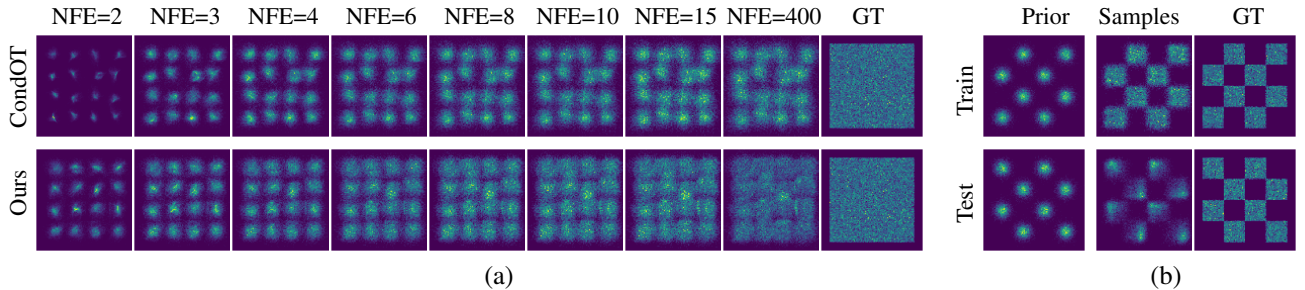


Figure 3. (a) **NFE convergence illustration.** A toy example illustrating convergence to the target distribution at different NFEs, for our method, compared to CondOT. (b). **Generalization illustration.** A toy example illustrating the generalization capabilities. LHS: Source prior and target samples for training classes RHS: As for LHS, but for test classes.

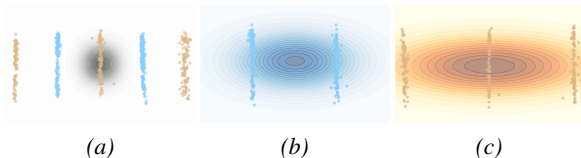


Figure 4. **Multi-modal classes.** A toy example illustrating multi-modal classes with intersections in the prior. Each color represents a class (class A or B), with samples as points and the prior distribution as contour lines. (a) shows a standard Gaussian prior (in black), while (b) and (c) show class-specific priors. While the mean each class falls on samples from the other class, our method results in an improved MMD score.

5. Experiments

We begin by validating our approach on a 2D toy example. Then, for two real-world datasets, we evaluate our approach on class-conditional and text-conditional image generation.

5.1. Toy Examples

We begin by considering the setting in which the prior distribution is a mixture of isotropic Gaussians (GMM), where each Gaussian’s mean represents the center of a class (we set the standard deviation to 0.2). The target distribution consists of 2D squares with the same center as the Gaussian’s mean in the source distribution and with a width and height of 0.2, representing a large square. We compare our method to class-conditional flow matching (with OT paths), where each conditional sample can be generated from each

Gaussian in the prior distribution.

In Fig. 2, we consider the trajectory from the prior to the target distribution. By starting from a more informative conditional prior, our method converges more quickly and results in a better fitting of the target distribution. In Fig. 3(a), we consider the resulting samples for the different NFEs. NFE indicates the number of function evaluation is used using a discrete Euler solver. Our method better aligns with the target distribution with fewer number of steps.

In Fig. 3(b), we consider the model’s ability to generalize to new classes not seen during training, akin to text-to-image generation’s setting. Training on only a subset of the classes our model exhibits generalization to new classes at test time.

In Fig. 4, we evaluate the method in the case where classes are not uni-modal and there are intersections in the prior distribution, following data from VLines of the Datasaurus Dozen (Gillespie et al., 2025). We present generated samples from a model trained using CondOT (a) alongside samples from our model (b, c). The maximum mean discrepancy (MMD) computed on this data is 0.084 for CondOT, while we achieve an improved MMD of 0.072.

5.2. Real World Setting

Datasets and Latent Representation Space. For the class-conditioned setting, we consider the ImageNet-64 dataset (Deng et al., 2009), which includes more than 1.28M training images and 50k validation images, categorized into

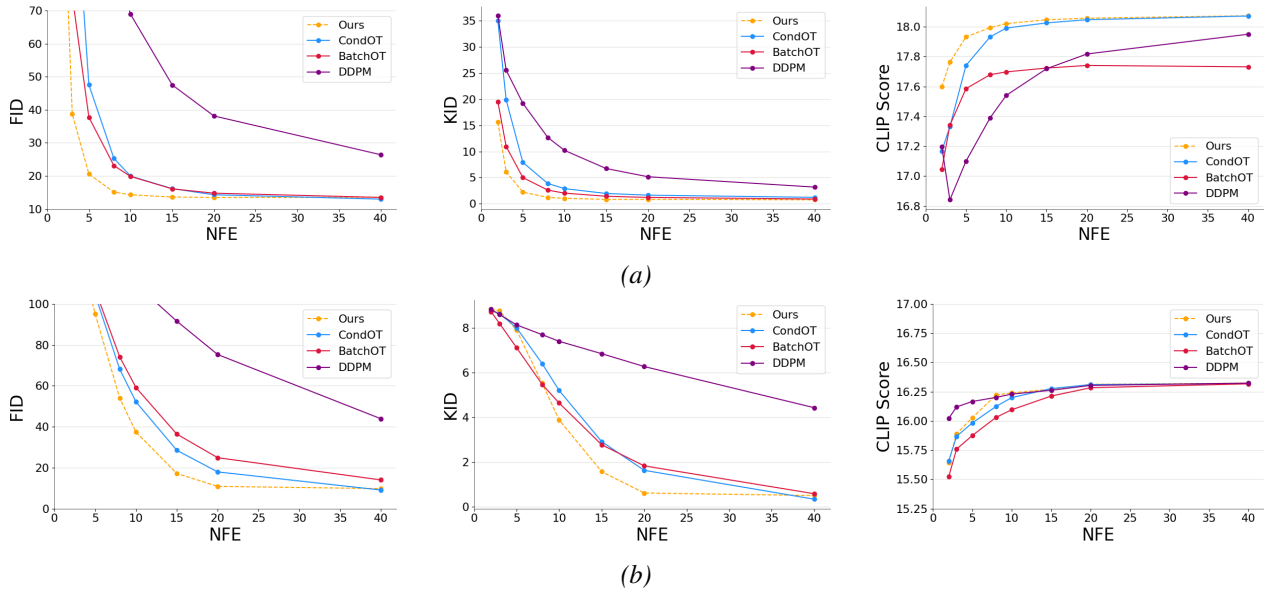


Figure 5. Numerical evaluation. (a) We compare our method to class conditional flow matching using optimal transport paths (CondOT) (Lipman et al., 2022), BatchOT (Pooladian et al., 2023), and DDPM (Ho et al., 2020a), on the ImageNet-64 dataset. We consider the FID score (LHS), KID score (Middle) and CLIP score (RHS). (b). As in (a) but for text-to-image generation on the MS-COCO dataset. As can be seen our method exhibit significant improvement per NFE, especially for low NFEs. For example, for 15 NFEs, on ImageNet-64 and MS-COCO we get **FID of 13.62** and **FID of 18.05** respectively, while baselines do not surpass FID of 16.10 and FID of 28.32 respectively for the same NFEs. We consider up to 40 NFE steps and note that DDPM converges to a superior result given more steps.

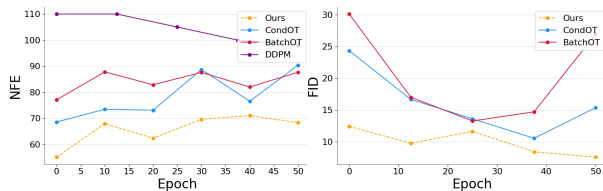


Figure 6. Training time. For a text-conditional model trained on MS-COCO, we consider the NFE per training epoch. We compare our method with text conditional flow matching using optimal transport paths (CondOT) (Lipman et al., 2022), BatchOT (Pooladian et al., 2023), and DDPM (Ho et al., 2020b). Note that DDPM had an FID value above 30 for all epochs so not shown on the RHS.

1k object classes, all resized to 64×64 pixels. For the text-to-image setting, we consider the 2017 split of the MS-COCO dataset (Lin et al., 2014), which consists of 330,000 images annotated with 80 object categories and over 2.5 million labeled instances. We use the standard split of 118k images for training, 5k for validation, and 41k for testing. We compute all our metrics on the ImageNet-64 validation set and the MS-COCO validation set. We perform flow matching in the latent representation of a pre-trained variational auto-encoder (van den Oord et al., 2018).

5.2.1. QUANTITATIVE RESULTS

For a fair comparison, we evaluate our method in comparison to baselines using the same architecture, training scheme, and latent representation, as detailed above. We compare our method to standard class-conditioned or text-



Figure 7. A visualization of our results on MS-COCO. We show, for four different text prompts: (a). The sample corresponding to the text in the conditional source distribution, which is used as the center of Gaussian corresponding to the text prompt (LHS) (b). Six randomly generated samples from the learned target distribution conditioned on the text prompt (RHS).

conditioned flow matching with OT paths (Lipman et al., 2022) which we denote CondOT, where the source distribution is chosen to be a standard Gaussian. We also consider BatchOT (Pooladian et al., 2023), which constructed a prior distribution by utilizing the dynamic optimal transport (OT) formulation across mini-batches during training. Lastly, we consider Denoising Diffusion Probabilistic Models (DDPM)

(Ho et al., 2020b). To evaluate image quality, we consider the KID (Bińkowski et al., 2021) and FID (Heusel et al., 2018) scores commonly used in literature. We also consider the CLIP score to evaluate the alignment of generated images to the input text or class, using the standard setting, as in (Hessel et al., 2022).

Overall Performance. We evaluate the FID, KID and CLIP similarity metrics for various NFE values (as defined above), which is indicative of the sampling speed. In Fig. 5(a) and Fig. 5(b), we perform this evaluation for our method and the baseline methods, for ImageNet-64 (class conditioned generation) and for MS-COCO (text-to-image generation), respectively. As can be seen, our method obtains superior results across all scores for both ImageNet-64 and MS-COCO. For ImageNet-64, already, at 15 NFEs our method achieves almost full convergence, whereas baseline methods achieve such convergence at much higher NFEs. This is especially true for FID, where our method converges at 15 NFEs, and baseline methods only achieve such performance at 30 NFEs. A similar behavior occurs for MS-COCO at 20 NFEs. We note that when considering NFEs for MS-COCO, we consider the pass in the mapper \mathcal{P}_θ to be marginal due to the small size of the the mapper in relation to the velocity v_θ , see Appendix C.

Training Convergence Speed. By starting from our conditional prior distribution, training paths are on average shorter, and so our method should also converge more quickly at training. To evaluate this, in Fig. 6, we consider the FID obtained at each epoch as well as the number of function evaluations (NFE) required for an adaptive solver to reach a pre-defined numerical tolerance, for a model trained on MS-COCO. Specifically, FID is computed using an Euler sampler with a constant number of function evaluations, NFE=20. As for the adaptive sampler, we use the dopri5 sampler with $\text{atol}=\text{rtol}=1\text{e-}5$ from the `torchdiffeq` (Chen, 2018) library. Our method results in lower NFEs and superior FID, for every training epoch.

Qualitative Results. In Fig. 7, we provide a visualization of our results for a model trained on MS-COCO. We show, for four different text prompts: (a). The sample corresponding to the text in the conditional source distribu-

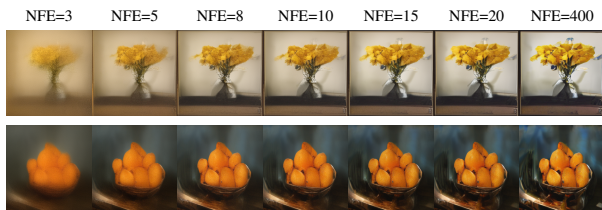


Figure 8. A visualization of our results for different NFEs. We consider a model trained on MS-COCO, and two different validation prompts: Top: “There are yellow flowers inside a vase”, Bottom: “A bowl full of oranges”.

tion, which is used as the center of Gaussian corresponding to the text prompt. (b). Six randomly generated samples from the learned target distribution conditioned on the text prompt. As can be seen, the conditional source distribution samples resemble ‘an average’ image corresponding to the text, while generated samples display diversity and realism. In the appendix, we also provide a diverse set of images generated by our method, in comparison to flow matching.

In Fig. 8, we consider, for a model trained on MS-COCO and a specific prompt, a visualization of our results for different NFEs, illustrating the sample quality for varying numbers of sampling steps. As can be seen, our method already produces highly realistic samples at NFE=15.

Table 2. **Ablation study.** Model performance for different values of σ (the standard deviation) as a hyperparameter for a model trained on MS-COCO. We also consider the case where our mapper \mathcal{P}_θ takes as input a bag-of-words encoding instead of a CLIP.

	FID ↓	KID ↓	CLIP ↑
$\sigma = 0.2$	23.55	2.88	16.12
$\sigma = 0.5$	15.47	0.93	15.75
$\sigma = 0.7$	7.55	0.61	15.85
$\sigma = 1.0$	7.87	1.66	15.81
w/o CLIP	16.33	2.38	15.51

Ablation Study. In the continuous setting, as in MS-COCO, our method requires choosing the hyperparameter σ , the standard deviation of each Gaussian. In Tab. 2, we report the FID, KID, and CLIP similarity values for different values of σ . As can be seen, our method results in best performance when $\sigma = 0.7$, we believe that a relative large σ is necessary to allow a richer conditional prior due to the complex nature of the conditional image distribution. We also consider the case where our mapper \mathcal{P}_θ takes as input a bag-of-words encoding instead of a CLIP encoding showing the importance of an expressive condition representation. As can be seen, performance drops significantly.

6. Conclusion

In this work, we introduce a novel initialization for flow-based generative models using condition-specific priors, improving both training time and inference efficiency. Our method allows for significantly shorter probability paths, reducing the global truncation error. Our approach achieves improved performance on MS-COCO and ImageNet-64, surpassing baselines in FID, KID, and CLIP scores, particularly at lower NFEs. The flexibility of our method opens avenues for further exploration of other conditional initialization. While this work we assumed a GMM structure of the prior distribution, different structures can be explored. Furthermore, one could incorporate additional conditions such as segmentation maps or depth maps.

References

- Albergo, M. S. and Vanden-Eijnden, E. Building normalizing flows with stochastic interpolants. *arXiv preprint arXiv:2209.15571*, 2022.
- Atanackovic, L., Zhang, X., Amos, B., Blanchette, M., Lee, L. J., Bengio, Y., Tong, A., and Neklyudov, K. Meta flow matching: Integrating vector fields on the wasserstein manifold, 2024. URL <https://arxiv.org/abs/2408.14608>.
- Bińkowski, M., Sutherland, D. J., Arbel, M., and Gretton, A. Demystifying mmd gans, 2021. URL <https://arxiv.org/abs/1801.01401>.
- Bull, L. A., Gardner, P., Rogers, T. J., Cross, E. J., Dervilis, N., and Worden, K. Probabilistic inference for structural health monitoring: New modes of learning from data. *ASCE-ASME Journal of Risk and Uncertainty in Engineering Systems, Part A: Civil Engineering*, 7(1), March 2021. ISSN 2376-7642. doi: 10.1061/ajrua6.0001106. URL <http://dx.doi.org/10.1061/AJRUA6.0001106>.
- Chen, R. T. Q. torchdiffeq, 2018. URL <https://github.com/rtqichen/torchdiffeq>.
- Chen, R. T. Q., Rubanova, Y., Bettencourt, J., and Duvenaud, D. Neural ordinary differential equations, 2019.
- Dao, Q., Phung, H., Nguyen, B., and Tran, A. Flow matching in latent space, 2023. URL <https://arxiv.org/abs/2307.08698>.
- Deng, J., Dong, W., Socher, R., Li, L.-J., Li, K., and Fei-Fei, L. Imagenet: A large-scale hierarchical image database. In *2009 IEEE conference on computer vision and pattern recognition*, pp. 248–255. Ieee, 2009.
- Dhariwal, P. and Nichol, A. Diffusion models beat gans on image synthesis. *Advances in neural information processing systems*, 34:8780–8794, 2021.
- Dilokthanakul, N., Mediano, P. A., Garnelo, M., Lee, M. C., Salimbeni, H., Arulkumaran, K., and Shanahan, M. Deep unsupervised clustering with gaussian mixture variational autoencoders. *arXiv preprint arXiv:1611.02648*, 2016.
- Esser, P., Kulal, S., Blattmann, A., Entezari, R., Müller, J., Saini, H., Levi, Y., Lorenz, D., Sauer, A., Boesel, F., et al. Scaling rectified flow transformers for high-resolution image synthesis. In *Forty-first International Conference on Machine Learning*, 2024.
- Gillespie, C., Locke, S., Davies, R., and D’Agostino McGowan, L. *datasauRus: Datasets from the Datasaurus Dozen*, 2025. URL <https://github.com/jumpingrivers/datasauRus>. R package version 0.1.9, <https://jumpingrivers.github.io/datasauRus/>.
- Hessel, J., Holtzman, A., Forbes, M., Bras, R. L., and Choi, Y. Clipscore: A reference-free evaluation metric for image captioning, 2022. URL <https://arxiv.org/abs/2104.08718>.
- Heusel, M., Ramsauer, H., Unterthiner, T., Nessler, B., and Hochreiter, S. Gans trained by a two time-scale update rule converge to a local nash equilibrium, 2018. URL <https://arxiv.org/abs/1706.08500>.
- Hinton, G. E. and Salakhutdinov, R. R. Reducing the dimensionality of data with neural networks. *science*, 313(5786):504–507, 2006.
- Ho, J. and Salimans, T. Classifier-free diffusion guidance. *arXiv preprint arXiv:2207.12598*, 2022.
- Ho, J., Jain, A., and Abbeel, P. Denoising diffusion probabilistic models. In Larochelle, H., Ranzato, M., Hadsell, R., Balcan, M., and Lin, H. (eds.), *Advances in Neural Information Processing Systems*, volume 33, pp. 6840–6851. Curran Associates, Inc., 2020a. URL https://proceedings.neurips.cc/paper_files/paper/2020/file/4c5bcfec8584af0d967f1ab10179ca4b-Paper.pdf.
- Ho, J., Jain, A., and Abbeel, P. Denoising diffusion probabilistic models. *Advances in neural information processing systems*, 33:6840–6851, 2020b.
- Isobe, N., Koyama, M., Zhang, J., Hayashi, K., and Fukumizu, K. Extended flow matching: a method of conditional generation with generalized continuity equation, 2024. URL <https://arxiv.org/abs/2402.18839>.
- Izmailov, P., Kirichenko, P., Finzi, M., and Wilson, A. G. Semi-supervised learning with normalizing flows. In *International conference on machine learning*, pp. 4615–4630. PMLR, 2020.
- Jiang, Z., Zheng, Y., Tan, H., Tang, B., and Zhou, H. Variational deep embedding: An unsupervised and generative approach to clustering, 2017. URL <https://arxiv.org/abs/1611.05148>.
- Kingma, D. P. and Ba, J. Adam: A method for stochastic optimization, 2017. URL <https://arxiv.org/abs/1412.6980>.
- Kobyzev, I., Prince, S. J., and Brubaker, M. A. Normalizing flows: An introduction and review of current methods. *IEEE transactions on pattern analysis and machine intelligence*, 43(11):3964–3979, 2020.

- Lee, S.-g., Kim, H., Shin, C., Tan, X., Liu, C., Meng, Q., Qin, T., Chen, W., Yoon, S., and Liu, T.-Y. Priorgrad: Improving conditional denoising diffusion models with data-dependent adaptive prior. *arXiv preprint arXiv:2106.06406*, 2021.
- Lin, T.-Y., Maire, M., Belongie, S., Hays, J., Perona, P., Ramanan, D., Dollár, P., and Zitnick, C. L. Microsoft coco: Common objects in context. *European conference on computer vision*, pp. 740–755, 2014.
- Lipman, Y., Chen, R. T., Ben-Hamu, H., Nickel, M., and Le, M. Flow matching for generative modeling. *arXiv preprint arXiv:2210.02747*, 2022.
- Liu, A. H., Le, M., Vyas, A., Shi, B., Tjandra, A., and Hsu, W.-N. Generative pre-training for speech with flow matching. In *The Twelfth International Conference on Learning Representations*, 2024. URL <https://openreview.net/forum?id=KpoQSgxbKH>.
- Liu, X., Gong, C., and Liu, Q. Flow straight and fast: Learning to generate and transfer data with rectified flow. *arXiv preprint arXiv:2209.03003*, 2022.
- McCann, R. J. A convexity principle for interacting gases. *Advances in Mathematics*, 128:153–179, 1997. URL <https://api.semanticscholar.org/CorpusID:123005604>.
- Papamakarios, G., Nalisnick, E., Rezende, D. J., Mohamed, S., and Lakshminarayanan, B. Normalizing flows for probabilistic modeling and inference. *Journal of Machine Learning Research*, 22(57):1–64, 2021.
- Pooladian, A.-A., Ben-Hamu, H., Domingo-Enrich, C., Amos, B., Lipman, Y., and Chen, R. T. Multisample flow matching: Straightening flows with minibatch couplings. *arXiv preprint arXiv:2304.14772*, 2023.
- Radford, A., Kim, J. W., Hallacy, C., Ramesh, A., Goh, G., Agarwal, S., Sastry, G., Askell, A., Mishkin, P., Clark, J., et al. Learning transferable visual models from natural language supervision. In *International conference on machine learning*, pp. 8748–8763. PMLR, 2021.
- Rombach, R., Blattmann, A., Lorenz, D., Esser, P., and Ommer, B. High-resolution image synthesis with latent diffusion models. In *Proceedings of the IEEE/CVF Conference on Computer Vision and Pattern Recognition*, pp. 10684–10695, 2022.
- Ronneberger, O., Fischer, P., and Brox, T. U-net: Convolutional networks for biomedical image segmentation, 2015. URL <https://arxiv.org/abs/1505.04597>.
- Sohl-Dickstein, J., Weiss, E., Maheswaranathan, N., and Ganguli, S. Deep unsupervised learning using nonequilibrium thermodynamics. In *International conference on machine learning*, pp. 2256–2265. PMLR, 2015.
- Song, Y., Sohl-Dickstein, J., Kingma, D. P., Kumar, A., Ermon, S., and Poole, B. Score-based generative modeling through stochastic differential equations. *arXiv preprint arXiv:2011.13456*, 2020.
- Süli, E. and Mayers, D. F. *An introduction to numerical analysis*. Cambridge university press, 2003.
- Tong, A., Malkin, N., Huguet, G., Zhang, Y., Rector-Brooks, J., Fatras, K., Wolf, G., and Bengio, Y. Improving and generalizing flow-based generative models with minibatch optimal transport. *arXiv preprint arXiv:2302.00482*, 2023.
- van den Oord, A., Vinyals, O., and Kavukcuoglu, K. Neural discrete representation learning, 2018. URL <https://arxiv.org/abs/1711.00937>.
- Vaswani, A., Shazeer, N., Parmar, N., Uszkoreit, J., Jones, L., Gomez, A. N., Kaiser, L., and Polosukhin, I. Attention is all you need, 2023. URL <https://arxiv.org/abs/1706.03762>.
- von Platen, P., Patil, S., Lozhkov, A., Cuenca, P., Lambert, N., Rasul, K., Davaadorj, M., Nair, D., Paul, S., Berman, W., Xu, Y., Liu, S., and Wolf, T. Diffusers: State-of-the-art diffusion models. <https://github.com/huggingface/diffusers>, 2022.
- Zheng, Q., Le, M., Shaul, N., Lipman, Y., Grover, A., and Chen, R. T. Q. Guided flows for generative modeling and decision making, 2023. URL <https://arxiv.org/abs/2311.13443>.

Table 3. **Numerical evaluation.** Quality of generated samples (FID, KID), and conditional fidelity (CLIP-Score) for our method in comparison to baselines, for the ImageNet-64 dataset for 15 NFEs. We consider CondOT (Lipman et al., 2022), BatchOT (Pooladian et al., 2023) and DDPM (Ho et al., 2020b).

	FID ↓	KID ↓	CLIP ↑
DDPM	47.51	6.74	17.71
CondOT	16.16	1.96	18.02
BatchOT	16.10	1.43	17.72
Ours	13.62	0.83	18.05

Table 4. Hyper-parameters used for training each model

	ImageNet-64	MS-COCO
Dropout	0.0	0.0
Effective Batch size	2048	128
GPUs	4	4
Epochs	100	50
Learning Rate	1e-4	1e-4
Learning Rate Scheduler	Constant	Constant

A. Additional Quantitative Results

In Tab.3, we present additional metrics (FID, KID, and CLIP-Score) for ImageNet-64 with 15 NFEs. We compare the performance of CondOT (Lipman et al., 2022), BatchOT (Pooladian et al., 2023) and DDPM (Ho et al., 2020b). As shown, our model delivers significant improvements over the baselines.

B. Visual Results

In Fig. 9, we provide additional visual results for our method in comparison to standard flow matching for a model trained on MS-COCO.

C. Implementation Details

We report the hyper-parameters used in Table 4. All models were trained using the Adam optimizer (Kingma & Ba, 2017) with the following parameters: $\beta_1 = 0.9$, $\beta_2 = 0.999$, weight decay = 0.0, and $\epsilon = 1e-8$. All methods we trained (*i.e.* Ours, CondOT, BatchOT, DDPM) using identical architectures, specifically, the standard Unet (Ronneberger et al., 2015) architecture from the `diffusers` (von Platen et al., 2022) library with the same number of parameters (872M) for the same number of Epochs (see Table 4 for details). For all methods and datasets, we utilize a pre-trained Auto-Encoder (van den Oord et al., 2018) and perform the flow/diffusion in its latent space.

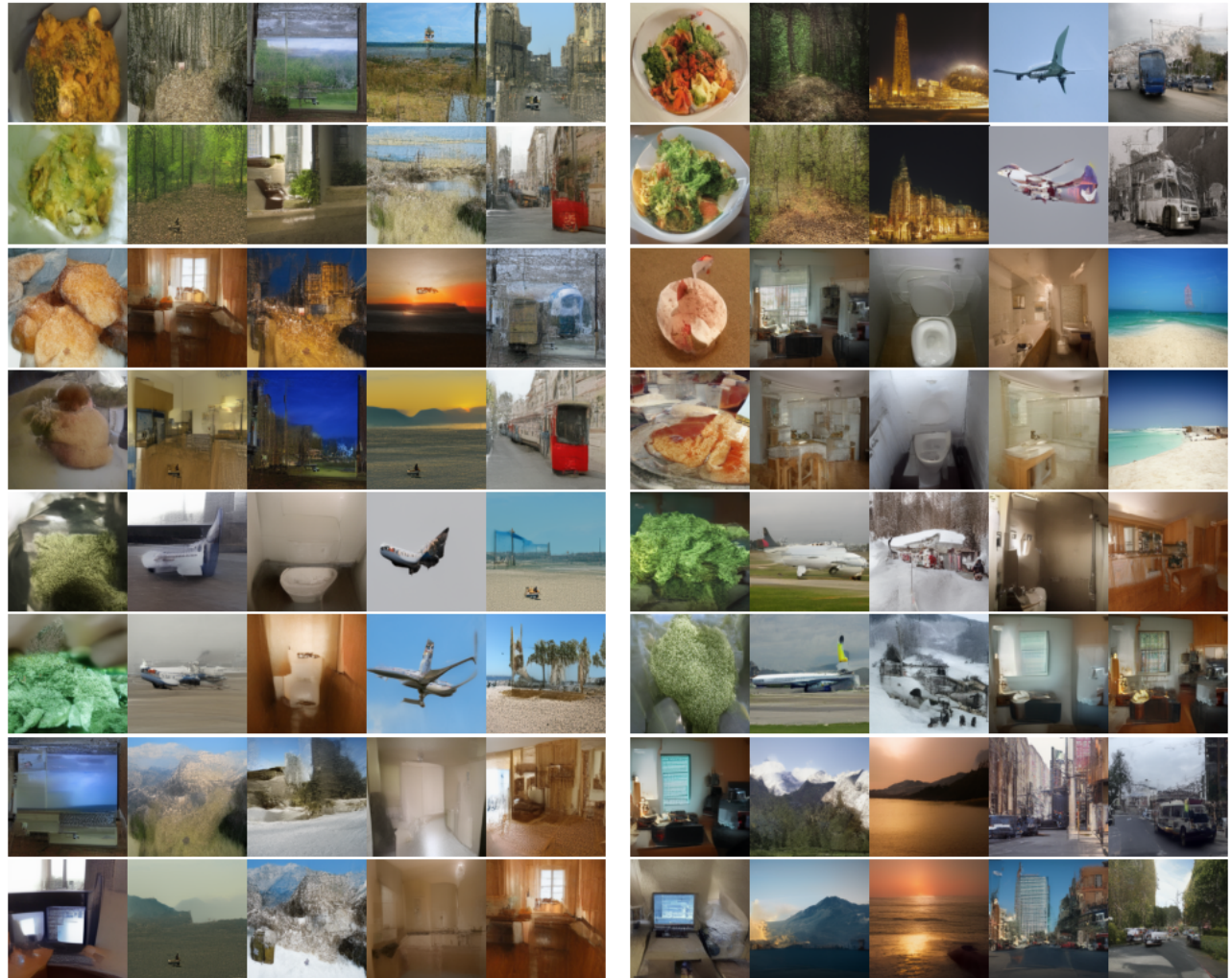
In the case of text-to-image generation, we encode the text prompt using a pre-trained CLIP network and pass to the

velocity v_θ using the standard UNet condition mechanism. In the class-conditional setting, we create the prompt ‘an image of a $\langle class \rangle$ ’ and use it for the same conditioning scheme as in text conditional generation.

For the mapper \mathcal{P}_θ from Sec 4.2 we use a network consisting a linear layer and 2 ResNet blocks with 11M parameters.

When using an adaptive step size sampler, we use `dopri5` with `atol=rtol=1e-5` from the `torchdiffeq` (Chen, 2018) library.

Regarding the toy example Sec. 5.1, we use a 4 layer MLP with ReLU activation as the velocity v_θ . In this setup, we incorporate the condition by using positional embedding (Vaswani et al., 2023) on the mean of each conditional mode and pass it to the velocity v_θ by concatenating it to its input.



Flow Matching

Ours

Figure 9. Visual comparison of randomly generated samples for prompts from the MS-COCO validation set using our method, in comparison to flow matching, for a model trained on MS-COCO.